Asian Journal of Engineering and Applied Technology
ISSN: 2249-068X (P) Vol. 5 No. 1, 2016, pp.29-35

DOI: https://doi.org/10.51983/ajeat-2016.5.1.769

Experimental Studies to Validate Computational Fluid Simulation of Coolant Flow Behavior through different Nozzles for Nozzle Effectiveness in Cylindrical Grinding Process to Enhance Workpiece Surface Quality

Mandeep Singh[1*], Yadwinderpal Sharma[2] and Jaskarn Singh[3]
[1& 2]Department of Mechanical Engineering, GZSCCET, Bathinda, Punjab, India
[3]Research Scholar, Department of Mechanical Engineering, UCOE, Punjabi University, Patiala, Punjab, India
* Corresponding author e-mail: smaghmandeep@gmail.com
(Received 21 March 2016; Accepted 19 April 2016; Available online 26 April 2016)

Abstract **- In the present paper, ANOVA (Analysis of Variance) technique has been adopted. The simulated results of flow behaviour through six different kinds of nozzles were experimentally validated to study the effect of these different types of nozzles as well as other process parameters on the response parameter namely surface roughness of ground workpiece during a cylindrical grinding process and optimized using this technique. The air flow behaviour around the rotating wheel and workpiece was simulated with computational fluid approach in ANSYS CFX. The optimum solution was found coherent with the simulated results. Spline type nozzle followed by convergent-divergent type was found the two best nozzles. Optimized solution also indicated the best parametric setting for the optimum results.**
Keywords: **ANOVA, Cylindrical grinding, flow behavior, workpiece, ANSYS CFX, nozzles, surface roughness**

I.INTRODUCTION

The increased temperature during grinding may affect the material properties and cause surface or subsurface cracks including burning along with residual stresses. Application of grinding fluid, therefore, is common during most grinding operations. The primary function of this fluid is to cool the workpiece and improve lubrication to reduce coefficient of friction between the wheel and the workpiece thus reducing the risk of thermal damage and improve process performance. The fluid also helps to wash away the chips and clean the machining area. The proper selection of a grinding fluid is an important process parameter along with method of application of the fluid to ensure effective cooling. The size and shape of the nozzle thus plays an important role to achieve these functional requirements of using the grinding fluid. Due to high rotational speed of grinding wheel, a thin air film layer surrounds the grinding wheel which restricts or even prevents the flow of the grinding fluid to the machining zone. This layer is often broken using a scraper board and the position of the scraper board is an important factor to consider.

A number of studies have been reported in the literature regarding the effect of heat on finish of a ground work piece. The temperature during the grinding process is significantly influenced by the process parameters and any change in such process parameters influences the amount of heat generated. Examination and comparison between dry and cutting fluid application (wet) in grinding to obtain best possible surface quality and dimensionally accurate ground parts have been made [1]. In most of the cases friction generated heat shortens tool life, increases surface roughness and lowers the dimensional sensitiveness of work material while machining difficult-to-cut materials [2, 3]. An overview of quantitative methods to calculate grinding temperature and the energy partition to the workpiece and concluded that cooling by the fluid at the grinding zone reduces the energy partition have been presented [4]. Investigations were made for the variation of the convection heat transfer coefficient (CHTC) of the process fluids within the grinding zone by using hydrodynamic and thermal modelling [5,6]. Jet impingement technology in a creep feed grinding process technique was used to spray the fluid normally at the grinding zone resulting in improved heat transfer to the fluid in relative comparison to conventional fluid delivery methods [7]. Theoretical model of fluid flow in grinding through a porous medium have been presented [8]. Investigations into air flow and particle distribution around grinding wheels have been made [9]. The effects of the boundary layer and effect of cutting fluid application method on grinding have been studied [10]. The quality of fluid required for grinding and the method of its application have been addressed [11].

New nozzle designs that give long coherent jets was presented, thus maximising the application of fluid into the grinding zone. The influences of nozzle position, jet velocity, and distance from the grinding zone have been studied. [12, 13]. Description of different methods for modelling and optimisation of grinding processes have been presented [14, 15]. The grind hardening process that utilises the heat dissipation in the grinding area for inducing metallurgical transformation on the surface of the ground workpiece have been analysed [16]. An improved thermal model which would accurately predict the position of the burn boundary has been developed [17]. In order to improve the efficiency of the grinding process, the fluid must be delivered in a manner that ensures that the jet velocity achieved via a nozzle provides adequate coverage of the grinding zone. The nozzle shape and geometry influences the fluid velocity and flow pattern at exit from the nozzle orifice [18]. Methods to determine the position of a coolant nozzle relative to a rotating grinding wheel along with an apparatus for practicing the method have been proposed

[19]. Also, new coolant nozzles and cooling methods have been proposed to reduce the grinding temperature, prevent the grinding wheel wear, and break the air layer in the grinding zone which prevents air suction from the sides and at the same time force the adequate fluid towards the grinding zone [20, 21]. Optimisation of cylindrical traverse grinding process whose objective is to maximize the material removal rate with constraints on workpiece out-of-roundness and waviness errors, on surface finish, and on grinding temperature have been reported [22]. Generalized intelligent grinding advisory system for the optimization of the three grinding processes: straight-cut surface grinding, internal and external cylindrical plunge grinding have been performed using fuzzy logic [23].

Improvement in design of delivery systems will require a detailed analysis of various nozzle shapes, their positioning and orientation with respect to the grinding wheel which have been undertaken in the present study. The optimum nozzle positioning angle is also dependent on jet speed/wheel speed ratio. Further, the fluid needs to be delivered in a manner that ensures the desired jet velocity and adequately coverage of the grinding zone. The jet velocity and the flow pattern at exit from the nozzle orifice are greatly influenced by nozzle geometry.

II. METHODOLOGY

In the present study, the air flow behavior around the rotating wheel and workpiece was simulated using different wheel and workpiece rotational speeds to calculate the maximum air velocity of the rotating air layer. Thereafter, six different shapes of nozzles were simulated to study the flow behavior and the maximum fluid velocity achieved through each nozzle. All the six nozzles were then experimentally tested on a cylindrical grinding machine to study their effect on workpiece surface finish.

TABLE 1 WHEEL AND OTHER DETAIL USED FOR SIMULATION

Grinding wheel	Technical Specification	A-60-L-5-V Specification (Al_2O_3 abrasive, medium grain size, medium grade, dense structure, vitrified bonding).
	Major dimensions	Outside diameter = 305 mm
		Internal bore diameter = 127 mm
		Width = 38 mm
Parameters used for simulation and boundary conditions	Workpiece diameter	15.5 mm
	Wheel rpm	1628, 1795, 1921
	Workpiece rpm	245, 375, 545
	Wheel roughness	1 mm
	Gap between wheel and workpiece	0.5 mm
	Ambient air properties	1 bar atmospheric pressure, standard atmospheric air properties at 25°C
	Coolant properties	Water, properties at 25°C

III. SIMULATION OF AIR FLOW BEHAVIOR AROUND ROTATING GRINDING WHEEL AND WORKPIECE

The air flow behavior around the grinding wheel was simulated using ANSYS CFX module. To replicate an actual profile of the grinding wheel, the wheel surface was treated as rough. Other parametric values used for the simulation are listed in Table 1. The simulation results showed that the velocity of surrounding air increased with increase in wheel velocity and decreased with increase in workpiece speed. Amongst the nine combinations of wheel and workpiece rotational speed (three rpm levels for wheel and workpiece each), the maximum velocity of air in the grinding zone was observed when the wheel and the workpiece rpm were set at 1921 rpm and 245 rpm respectively as shown in Fig. 1. The maximum velocity of 20.1 m/sec was observed. It can be concluded that in order to ensure effective cooling, the fluid velocity should be sufficiently high to break the rotating air layer.

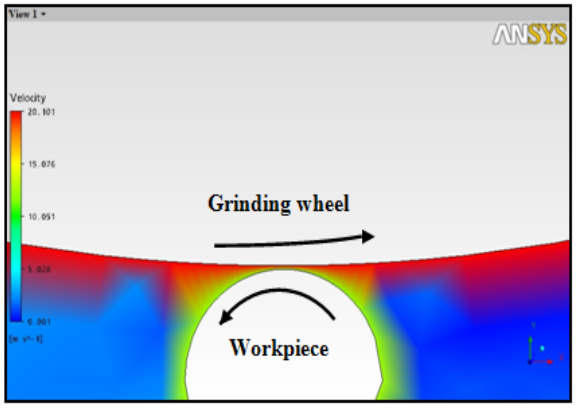

Fig. 1. Velocity contour around the grinding wheel and work piece in a cylindrical grinding process with (wheel revolution: 1921 rpm, workpiece revolution: 245 rpm)

IV.DESIGN OF NOZZLES AND GRINDING FLUID FLOW SIMULATION

Six different shapes of nozzles were considered for simulation study to identify the most appropriate nozzle using ANSYS CFX module. The shape and cross-sectional geometry of these nozzles is given in Fig. 2. Any further increase or decrease in nozzle exit diameter would reduce the exit velocity or reduce the volume which would be insufficient to cover the grinding zone. The inlet diameter of the nozzle was selected to have sufficient pressure of the fluid. With diameter less than 25 mm, fluid pressure was observed to be high thereby resulting in high fluid velocity with low volume of fluid. With increase in inlet diameter, fluid pressure dropped than the required condition.

Simulations of flow behavior using each of the six nozzles are shown from Fig. 3. For each of the six nozzles, it was observed that the peak velocity of the fluid was achieved after the fluid flushes out of the nozzle and velocity drops as it travels longer distance thereafter. The

location at which the peak fluid velocity was obtained was used to set the gap between the nozzle and the wheel. The other requirement was to ensure that the peak fluid velocity is higher than that of the air velocity circumscribing the grinding wheel in order to break this layer. The location at which the peak fluid velocity was obtained was used to set the gap between the nozzle and the wheel. The other requirement was to ensure that the peak fluid velocity is higher than that of the air velocity circumscribing the grinding wheel in order to break this layer.

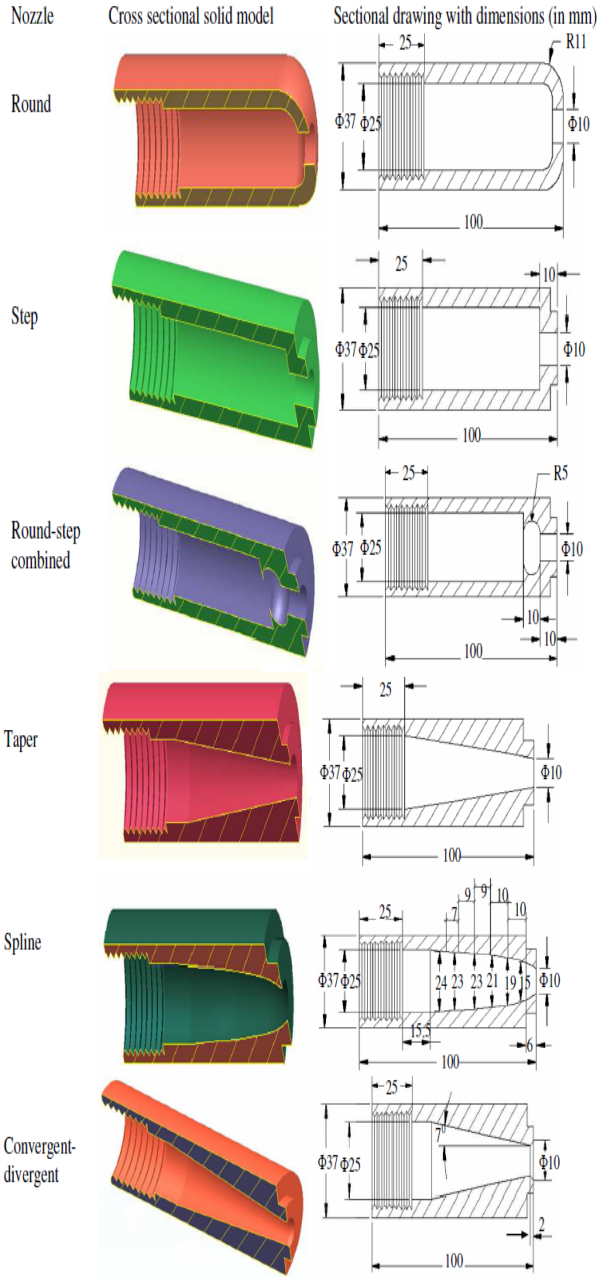

Fig. 2 Six different kinds of nozzles used for simulation and experimentation (dimensions not to scale)

Fig. 3 (a) shows the vector plot respectively, at the exit side of a round nozzle. Peak fluid velocity achieved is high but the stream of fluid was observed to be inclined towards one side. Also, the velocity remains sufficiently high even for a substantial distance from the nozzle exit. Fig. 3 (b) shows the flow behavior for a stepped nozzle.

Maximum fluid velocity in this case was observed slightly higher than the round shaped nozzle but drops considerably as the fluid travels a short distance from the nozzle exit. Also, the drop in velocity is continuous. Simulation of flow through the round-step combined nozzle is shown in Fig. 3 (c). Peak fluid velocity through this nozzle was found to be least amongst the six shapes considered in the simulation study. There is a sudden drop in fluid velocity after the nozzle exit but thereafter a gradual drop was observed. This could be due to the round region just before the nozzle exit which has a tendency to push the fluid stream towards the centre. As the fluid from all sides of circumferential shape of nozzle meet at the centre of flow, the droplets collide and collapse resulting in a large drop in fluid velocity. Flow behavior of fluid through a taper nozzle is shown in Fig. 3 (d). Fluid through this nozzle attains a higher flow velocity than the previous three cases. After exit from the nozzle the fluid velocity reaches the maximum at a very short distance from the nozzle exit and then decreases gradually. Fig. 3 (e) shows flow behavior of fluid passing through a convergent-divergent nozzle. In this case, peak fluid velocity achieved after the exit of the nozzle is higher than round, step or round-step combined, and taper but lower than the spline shaped nozzle.

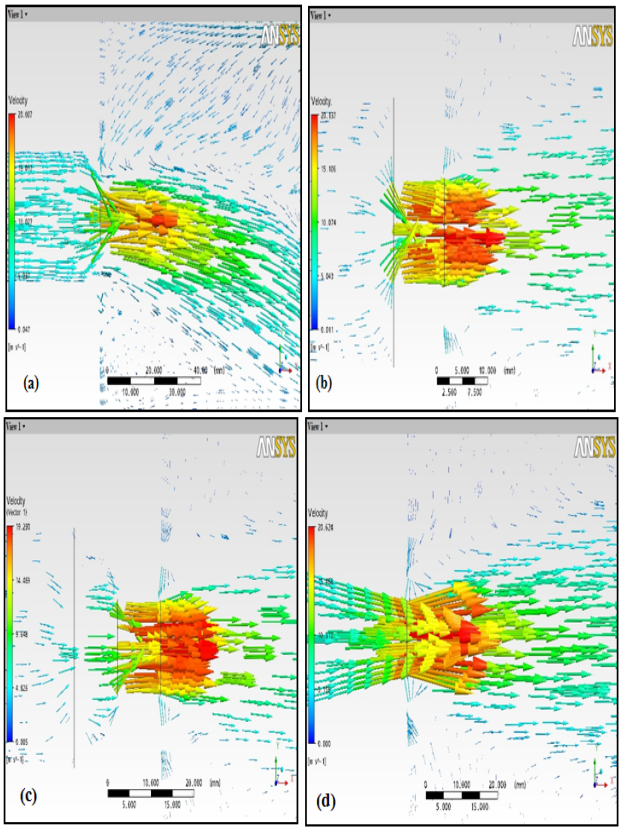

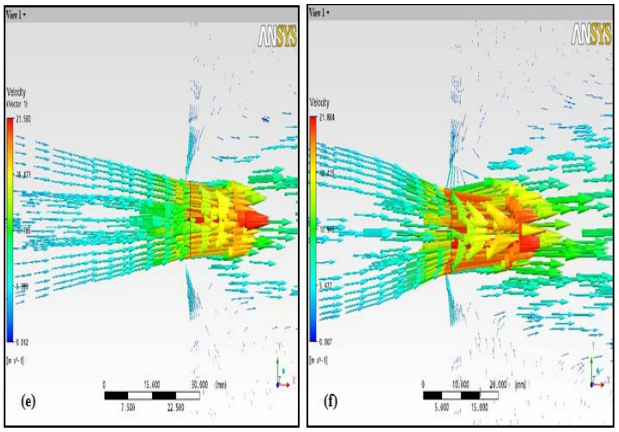

Figure 3. Pattern of fluid flow velocity vector from different nozzles, (a) round nozzle (b) step nozzle (c) round-step combined nozzle (d) taper nozzle (e) convergent-divergent nozzle (f) spline nozzle

The fluid velocity drops at a short distance after the exit and stabilizes with little drop in velocity thereafter. Fig. 3 (f) shows the fluid flow velocity vector obtained with a nozzle with spline cross section. The peak fluid velocity achieved in this case was highest as compared to the other five shapes. A marginal drop in fluid velocity was observed after the exit and negligible drop was noticed afterwards indicating a small decrease over the travel region. The peak velocity achieved in this case was highest and was also maintained for a sufficiently long distance from the exit. Based on the above discussion, it can be concluded that the fluid through a nozzle with a spline cross-section would be the best suited to effectively break the rotating air layer and is also likely to cover the largest area in the grinding zone. The spline and convergent-divergent shaped nozzles were thus observed to be the two best nozzles in that order with high peak fluid velocity in relative comparison to four other commonly used shapes. The highest value of peak fluid velocity with each of the six nozzles is given in Table 2.

TABLE 2. PEAK VELOCITIES ACHIEVED THROUGH DIFFERENT NOZZLES

Nozzle type	**Peak velocity (m/s)**
Round	20.007
Step	20.137
Round-step combined	19.290
Taper	20.624
Spline	21.884
Convergent-divergent	21.560

V. EXPERIMENTAL DESIGN

The experimental study was undertaken with an objective to validate the results of the simulation study described in the above section. With the simulated results available, the experimental study was undertaken to evaluate the effect of different nozzle geometrical shapes, wheel and workpiece speed, nozzle tip distance and nozzle orientation angle in cylindrical grinding on surface roughness. Other factors such as type of grinding fluid, fluid pressure, workpiece material, and grinding wheel grade were kept constant during the experimental study. The levels for the machine parameters like wheel speed, workpiece speed were selected as per the pulley combinations available on the cylindrical grinder. The nozzle tip distance and orientation angle were selected based on the results of the simulation study as well as other studies reported in literature. Based on the above discussion, six different combinations of nozzle geometrical shapes (based on simulation study) and three levels each of the other factors were selected for the experimental study. The various levels for the control factors, thus selected for experimentation during the study are listed in Table 3 six different nozzle shapes namely round-step combined, round, spline, convergent-divergent, taper and step cross sections had the same dimensions as used in simulation study and were manufactured using a Aluminum-Magnesium-Silicon alloy. The nozzles were bored to the required size as shown in Fig. 2 and finished by a profile tool to the desired shape. The grinding fluid was pumped with the help of a centrifugal pump at a pressure of 3 bar maintained with a regulating valve. Pressure was measured with the help of a mercury manometer. The fluid was pumped from a sump tank of 100 liter capacity. The schematic arrangement is shown in Fig. 4. The speed of the wheel and workpiece was varied by changing belts on various pulley combinations. The nozzle tip distance and the nozzle orientation angle were varied using a screw arrangement. The nozzle angle with the vertical was measured using a scraper with angle markings.

TABLE 3. FACTORS AND THEIR LEVELS STUDIED FOR THE EXPERIMENTATION

Factors *(units)*	*Levels*					
	Level 1	*Level 2*	*Level 3*	*Level 4*	*Level 5*	*Level 6*
Nozzle type, NT	Round-step combined	Round	Spline	Convergent-divergent	Taper	Step
Wheel Speed, V (m/sec)	25.98	28.65	30.66			
Workpiece Speed, v (m/sec)	0.198	0.304	0.442			
Nozzle tip distance, D (mm)	6	12	18			
Nozzle angle, α (degrees)	18	25	32			

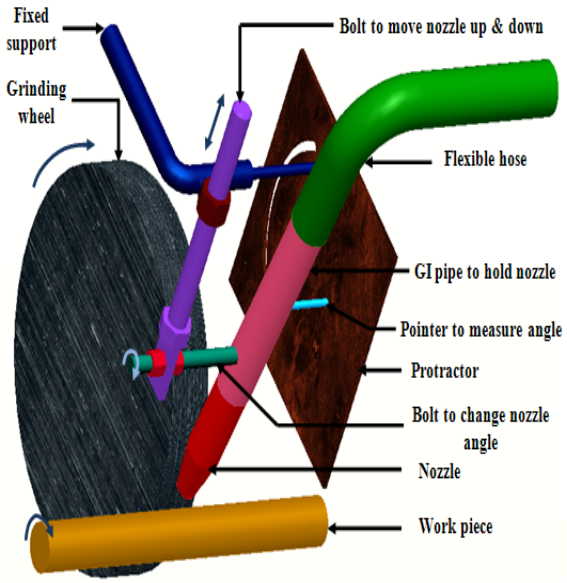

Fig.4 Detail of arrangement for nozzle setting

VI. EXPERIMENTAL SETUP AND PROCEDURE

The experiments were conducted on the Cylindrical Grinding Machine. The workpiece material of plain carbon steel and alumina abrasive (Al_2O_3) grinding wheel (specification: A-60-L-5-V) were used during the experimental study. The experimental design was completed using the Taguchi's Fractional Factorial Experiments (FFEs) [24]. In the present experimental situation, five factors were varied during the experiment. Each of the three level factors (wheel speed, workpiece speed, nozzle tip angle and nozzle tip distance), have two degrees of freedom (dof) associated with them. The one factor (nozzle shape) varied at six levels has five dof. The total dof required for designing an orthogonal experiment for the present study were thus calculated to be 13. A possible array for studying a combination of a six-level and three-level factors is an eighteen trial Orthogonal Array labeled as L_{18} matrix shown in Table 5. The assignment of factors was completed using the Taguchi Linear Graphs and Triangular Tables [24] in combination with MINITAB 15, a statistical software to aid this analysis.

Eighteen workpieces of length 290 mm were cut from a 20 mm diameter plain carbon steel rod. The parts were turned to a diameter of 15.6 mm and were then finished to the required diameter of 15.5 mm on the cylindrical grinder used during the experimental study. Four finishing cuts on each piece were undertaken on the grinder. The first two passes were made with a depth of cut of 0.15 mm and the final two passes were machined with 0.10 mm depth of cut each.

The surface roughness was measured at six pre-determined positions on the workpiece after each trial C_{pk} of which is listed in Table 4. Four measurements for surface roughness R_a was taken at each of these six positions and were averaged to obtain the central tendency for detailed statistical analysis.

VII. PROCESS CAPABILITY (C_{PK}) ANALYSIS

Six grinding cuts were made during each of the 18 trials. Five measurements were taken for surface roughness at each of the six cuts after each trial. Therefore, 30 measurements were taken during each trial which is a sufficient sample size for process capability assessment. The Process Capability Index C_{pk} was obtained by calculating the standard deviation (σ, a measure of process variation) using equation 1. The C_{pk} was then calculated by comparing the 3σ limits with the part tolerance for outside diameter as well as surface roughness using equation 2.

$$\sigma = \sqrt{\sum_{i=1}^{n} \frac{\left(x_i - \bar{x}\right)^2}{n-1}} \qquad \text{……Eqn. (1)}$$

$$C_{pk} = \text{minimum of } \frac{U_{SL} - \bar{x}}{3\sigma} \text{ and } \frac{\bar{x} - L_{sl}}{3\sigma}$$

(should be > 1.33) …… Eqn. (2)

Where n is the number of replications, x_i is the value of the output (finish diameter or surface roughness) at *i*th interval and $\bar{x}$ is the arithmetic mean.
Process capability index is given by equation (2)
Where U_{SL} is the Upper Specification Limit and L_{SL} is the Lower Specification Limit, $\bar{x}$ is the arithmetic mean and σ is the standard deviation of the measurements. The C_{pk} value is taken as minimum of the two in Equation (2).

Surface roughness has a unilateral tolerance and needs to be controlled for an absolute value along with process variation. C_{pk} index includes both the absolute value of roughness (measured in terms of $\bar{x}$) as well as process variation (measured in terms of σ) and was used to assess the capability of maintaining a better surface finish.

All the parts produced after completion of each of the eighteen trials were measured for surface roughness (specification: maximum 0.0012 mm). In this case the specifications for roughness were taken as maximum 1.2 µm and it is common to have this limited to 0.8 µm. The lowering of the specification range will lower the C_{pk} value. The statistical calculations and the plots were compiled using the MINITAB15 statistical software. The results for C_{pk} for surface roughness achieved after grinding at six different positions for each trial is shown in Table 5. The results were analyzed using Analysis of Variance (ANOVA) for identifying the significant factors affecting the performance measures.

VIII. RESULTS AND ANALYSIS

The ANOVA data for C_{pk} of surface roughness is given in Table 5. The ANOVA results for surface roughness showed that the nozzle shape and nozzle tip distance were

the most significant factors. All the remaining factors were found to be insignificant.

The main effect plots for capability index for surface roughness are shown in Fig. 5. One can observe from Fig. 5 and Table 5, that a high process capability index for surface roughness is achieved when a spline shaped nozzle set at a tip distance of 18 mm is used. One trial where the nozzle tip distance was 6 mm, the capability index dropped to less than desired value of 1.33. Also, in all the trials where the tip distance was set at 6 mm, the process capability index for surface finish dropped to a negative value indicating a very poor capability to hold the tolerance.

This is perceived to be due to the high impact of the fluid jet which may induce vibrations on the workpiece surface thereby affecting the finish. However, the lowest setting of the nozzle tip distance did not cause poor capability as was the case in surface roughness calculations. This is potentially a conflict situation which may be controlled by setting the nozzle tip distance at its highest level (18 mm) where the capability for both the parameters was observed to be high. Optimal nozzle geometry is likely to improve the cooling efficiency of the process resulting in quick dissipation of heat during grinding. The fluid also washes away the chips from the grinding zone thereby reducing the effect of wheel loading. The embedment of chips leads to a smooth and shiny wheel surface that ceases to cut effectively causing poor finish on the workpiece. Further, due to wet grinding the coefficient of friction between the wheel and the workpiece is reduced which improves the finish. The overall impact of these improvements leads to an improved process capability.

TABLE 4. L_{18} EXPERIMENTAL DESIGN IN TERMS OF LEVEL SYMBOLS AND RESULTS OF SURFACE ROUGHNESS R_A

Trial number	Nozzle type	Wheel speed	Work-piece speed	Nozzle tip distance	Nozzle angle	C_{pk} of Surface Roughness R_a (µm)
1.	Round-step combined (NT_1)	V_1	v_1	D_1	α_1	0.75
2.	Round-step combined (NT_1)	V_2	v_2	D_2	α_2	1.86
3.	Round-step combined (NT_1)	V_3	v_3	D_3	α_3	2.85
4.	Round (NT_2)	V_1	v_1	D_2	α_2	-0.9
5.	Round (NT_2)	V_2	v_2	D_3	α_3	0.76
6.	Round (NT_2)	V_3	v_3	D_1	α_1	-0.58
7.	Spline (NT_3)	V_1	v_2	D_1	α_3	-0.27
8.	Spline (NT_3)	V_2	v_3	D_2	α_1	7.65
9.	Spline (NT_3)	V_3	v_1	D_3	α_2	8.16
10.	Convergent-divergent (NT_4)	V_1	v_3	D_3	α_2	2.4
11.	Convergent-divergent (NT_4)	V_2	v_1	D_1	α_3	-0.52
12.	Convergent-divergent (NT_4)	V_3	v_2	D_2	α_1	-0.44
13.	Taper (NT_5)	V_1	v_2	D_3	α_1	0.32
14.	Taper (NT_5)	V_2	v_3	D_1	α_2	-0.47
15.	Taper (NT_5)	V_3	v_1	D_2	α_3	0.46
16.	Step (NT_6)	V_1	v_3	D_2	α_3	-0.56
17.	Step (NT_6)	V_2	v_1	D_3	α_1	-1.2
18.	Step (NT_6)	V_3	v_2	D_1	α_2	-0.64

TABLE 5. ANALYSIS OF VARIANCE FOR MEANS OF C_{PK} OF SURFACE ROUGHNESS (RA)

Source	Degree of freedom	Sum of squares	Variance	F-test value	Percentage Contribution
Nozzle type	5	71.925	14.385	3.48	56.8
Wheel speed	2	6.029	3.014	0.73	4.76
Work-piece speed	2	7.862	3.931	0.95	6.21
Nozzle tip distance	2	19.349	9.675	2.34	15.28
Nozzle angle	2	4.922	2.461	0.59	3.88
Residual Error	4	16.554	4.138		13.07
Total	17	126.641			100

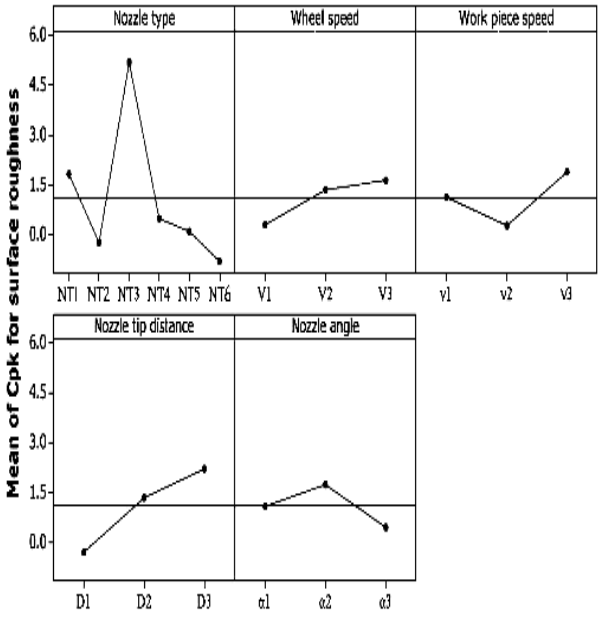

Fig.5 Main effects plot for means of C_{pk} of surface roughness (Ra)

IX. CONCLUSIONS

In this study, the computational fluid simulation approach (using ANSYS CFX module) has been successfully applied to study the behavior of air flow around grinding wheel and workpiece during a cylindrical grinding process. Further, six different nozzle geometrical shapes were simulated to study the fluid flow velocity and its distribution profile in the grinding zone after exit from the nozzle. Based on the simulated results, it was concluded that for effectively breaking the thin layer of air that circumscribes the rotating wheel, the peak fluid velocity should be more than 20.1 m/sec. This will result in more effective cooling of the workpiece which directly affects the capability to hold dimensional specifications as well as provide superior finish. It was further concluded that nozzles with a spline or a convergent-divergent cross-section will provide the maximum fluid velocity thus overcoming the air film around the wheel and more effective cooling.

The simulation results were validated experimentally using Taguchi's design. The experimental results matched with the simulation results to show best results in holding process specifications using a spline shaped nozzle followed by a convergent-divergent shaped nozzle. The experimental study was also helpful in establishing the nozzle tip distance which should be set at 18 mm for improved process capability of maintaining the size and lowering the surface roughness.

REFERENCES

[1] Kiyak, M. and Cakir, O. (2010), "Study of surface quality in dry and wet external cylindrical grinding", *Int. J. Compu. Mater. Sci. Surf. Engg.*, Vol. 3, No. 1, pp.12–23.

[2] Silva, M.B. Da and Wallbank, J. (1998), "Lubrication and application method in machining", *Industrial Lubrication and Tribology*, pp. 149-152.

[3] Cakir, O., Yardimeden, A., Ozben T. and Kilickap, E. (2007),"Selection of cutting fluids in machining processes"*Journal of Achievements in Materials & Manufacturing Engineering*, pp. 99-102.

[4] Guo, C. and Malkin, S. (2000), "Energy partition and cooling during grinding", *J. Manuf. Processes*, Vol. 2, No. 3, pp.151–157.

[5] Jin, T., Stephenson, D.J. and Rowe, W.B. (2003), "Estimation of the convection heat transfer coefficient of coolant within the grinding zone", *Proc. I. Mech. E., Part B: J. Engineering Manufacture*, Vol. 217, No. 3, pp.397–407.

[6] Jin, T. and Stephenson, D.J. (2008), "A study of the convection heat transfer coefficients of grinding fluids", *CIRP Annals – Manuf. Technol.*, Vol. 57, No. 1, pp.367–370.

[7] Sun, F. H.; Xu, H. J. (2002), "A new technology on enhancing heat transfer at grinding zone through jet impingement during creep feed grinding",*Machining Science and Technology*, pp.372-384.

[8] Guo, C.; Malkin, S. (1992), "Analysis of fluid flow through the grinding zone", *Journal of Engineering Industry-Transactions of ASME*, pp.427–434

[9] Davies, T.P.; Jackson, R.G. (1981), "Air flow around grinding wheels", *Journal of Precision Engineering*, pp.225 228.

[10] Ebbrell, S.; Woolley, N.H.; Tridimas, Y.D.; Allanson, D.R.; Rowe, W.B. (2000), "The effects of cutting fluid application methods on the grinding process", *International Journal of Machine Tools & Manufacture*, pp. 209-223.

[11] Morgan, M.N.; Jackson, A.R.; Wu, H.; Baines-Jones, V.; Batako, A.; Rowe, W.B. (2008), "Optimization of fluid application in Grinding", *CIRP Annals – Manufacturing Technology*, pp. 363-366.

[12] Webster, J.A.; Cui, C.; Mindek Jr. R.B.; Lindsay, R.(1995), "Grinding fluid application system design" ,*CIRP Annals–Manufacturing Technology*, pp.333-338.

[13] Webster, J.A.; Storrs, C.T. (2006), "Coherent jet nozzles for grinding applications", *US Patent Application Publication, Publication number: US2006/7086930 B2, Saint-Gobain Abrasives, Inc., August 2006.*

[14] Brinksmeier, E.; Tonshoff, H.K.; Czenkusch, C.; Heinzel, C. (1998), "Modelling and optimization of grinding processes", *Journal of Intelligent manufacturing*, pp. 303-314.

[15] Brinksmeier, E.; Aurich, J.C.; Govekar, E.; Heinzel, C.; Hoffmeister, H.W.; Klocke, F.; Peters, J.; Rentsch, R.; Stephenson, D.J.; Uhlmann, E.; Weinert, K.; Wittmann, M. (2006), "Advances in modeling and simulation of grinding processes", *CIRP Annals – Manufacturing Technology*, pp. 667-696.

[16] Salonitis, K. and Chryssolouris, G. (2007), "Cooling in grind-hardening operations", *Int. J. Adv. Manuf. Technol.*, Vol. 33, Nos. 3–4, pp.285–297

[17] Rowe, W.B., Pettit, J.A., Boyle, A. and Moruzzi, J.L. (1998), "Avoidance of thermal damage in grinding and prediction of the damage threshold", *CIRP Annals – Manuf. Technol*, Vol. 37, No. 1, pp.327–330.

[18] Morgan, M.N.; Baines-Jones, V. (2009), "On the Coherent Length of Fluid Nozzles in Grinding", *Key Engineering Materials–Progress in Abrasive and Grinding Technology*, pp. 61-67.

[19] Pilkington, M.I. (2009), "Coolant nozzle positioning for machining work-pieces", *US Patent, Patent number: US2009/7568968 B2, Rolls-Royce Corporation.*

[20] Shin'ichi, N.; Shin'ichi, T. (2000), "Development of coolant method applied formed grinding, Test and performance evaluation of floating nozzle', *Journal of Japan Society for Precision Engineering*, pp.865-870.

[21] Banerjee, S.; Ghosal, S.; Dutta, T. (2008), "Development of a simple technique for improving the efficacy of fluid flow through the grinding zone", *Journal of Materials Processing Technology*, pp. 306-313.

[22] Kruszyński, B.W. and Lajmert, P. (2006), "An intelligent system for online optimization of the cylindrical traverse grinding operation", *Proc. I. Mech. E., Part B: J. Engineering Manufacture*, Vol. 220, No. 3, pp.355–363.

[23] Vishnupad, P. and Shin, Y.C. (1998), "*Intelligent* optimization of grinding processes using fuzzy logic", *Proc. I. Mech. E., Part B: J. Engineering Manufacture*, Vol. 212, No. 8, pp.647–660.

[24] Ross, Phillip J. (1995), "Taguchi Techniques for Quality Engineering", *Mc Graw-Hill Book Company, Second Edition.*